Direct Evidence for Solid-Like Hydrogen in a Nanoporous Carbon Hydrogen Storage Material at Supercritical Temperatures

Valeska P. Ting *[†], Anibal J. Ramirez-Cuesta [§], Nuno Bimbo [†], Jessica E. Sharpe [†], Antonio Noguera-Diaz [†], Volker Presser[‖][‡], Svemir Rudic[¶], Timothy J. Mays [†]

[†] Department of Chemical Engineering, University of Bath, Bath BA2 7AY, United Kingdom
[§] Chemical and Engineering Materials Division, Oak Ridge National Laboratory, Oak Ridge, Tennessee 37831-6475, United States of America
[‖] INM – Leibniz Institute for New Materials, Campus D2 2, 66123 Saarbrücken, Germany
[‡] Department of Materials Science and Engineering, Saarland University, Campus D2 2, 66123 Saarbrücken, Germany
[¶] ISIS Facility, STFC, Rutherford Appleton Laboratory, Didcot OX11 0QX, United Kingdom

Supporting Information Placeholder

ABSTRACT: Here we report direct physical evidence that confinement of molecular hydrogen (H_2) in an optimized nanoporous carbon results in accumulation of hydrogen with characteristics commensurate with solid H_2 at temperatures up to 67 K above the liquid-vapour critical temperature of bulk H_2. This extreme densification is attributed to confinement of H_2 molecules in the optimally-sized micropores, and occurs at pressures as low as 0.02 MPa. The quantities of contained, solid-like H_2 increased with pressure and were directly evaluated using *in-situ* inelastic neutron scattering and confirmed by analysis of gas sorption isotherms. The demonstration of the existence of solid-like H_2 challenges the existing assumption that supercritical hydrogen confined in nanopores has an upper limit of liquid H_2 density. Thus, this new insight offers new opportunities for the development of more accurate models for the evaluation and design of nanoporous materials for high capacity adsorptive hydrogen storage.

Molecular hydrogen (H_2) has excellent potential as a sustainable, low-carbon and non-polluting energy vector. However, above its bulk liquid-vapour critical temperature of 33 K,[1] hydrogen exists as a gas, and will not form a higher-density bulk liquid or a solid, except under extreme conditions of high pressure (*e.g.,* > 5 GPa).[2,3] Subsequently, the efficient and economic storage of molecular H_2 remains a major technological challenge.[4,5] One option for increasing storage densities is *via* adsorption of H_2 into microporous materials, that is, materials with pore diameters < 2 nm[6]. In such mate-rials, densification of H_2 is promoted *via* the enhancement of the attractive van der Waals interactions between adsorbed H_2 molecules and the solid substrate, arising from overlapping potentials from opposite pore walls. Evaluation of gas storage capacities of promising nanoporous materials generally involves measurement of the Gibbs excess uptake *via* isothermal gas sorption, with the subsequent conversion of the excess to absolute H_2 uptake requiring an estimate of the adsorbed hydrogen density.[7] As the density of H_2 inside the micropores is difficult to probe experimentally, the maximum (limiting) density of H_2 is generally approximated to be the same as liquid hydrogen (*i.e.,* a uniform density of ~77 kg m^{-3} at the triple point), despite temperatures of adsorptive storage typically exceeding the bulk critical temperature.[8] One of the few experimental techniques that can directly access information on the state of the adsorbed H_2 inside a porous material and potentially validate the assumption of liquid-like adsorbed phase densities is neutron scattering. Neutrons are highly sensitive to ^{1}H due to its large incoherent neutron scattering cross section. While there have been numerous neutron diffraction studies investigating the binding of hydrogen to strong adsorption sites in metal-organic frameworks (MOFs),[9,10,11] due to the magnitude of the incoherent scattering background, [1]H_2 is almost always substituted by D_2. The differences in molecular weights may introduce isotope effects that will affect bond distances, vibrational energies and packing densities. To avoid the need for deuteration and to allow investigation of non-crystalline materials, in this study we used inelastic neutron scattering (INS), a technique that is not hampered by the ^{1}H incoherent

scattering and which measures vibrational motions and thus the binding strength of atoms and molecules.
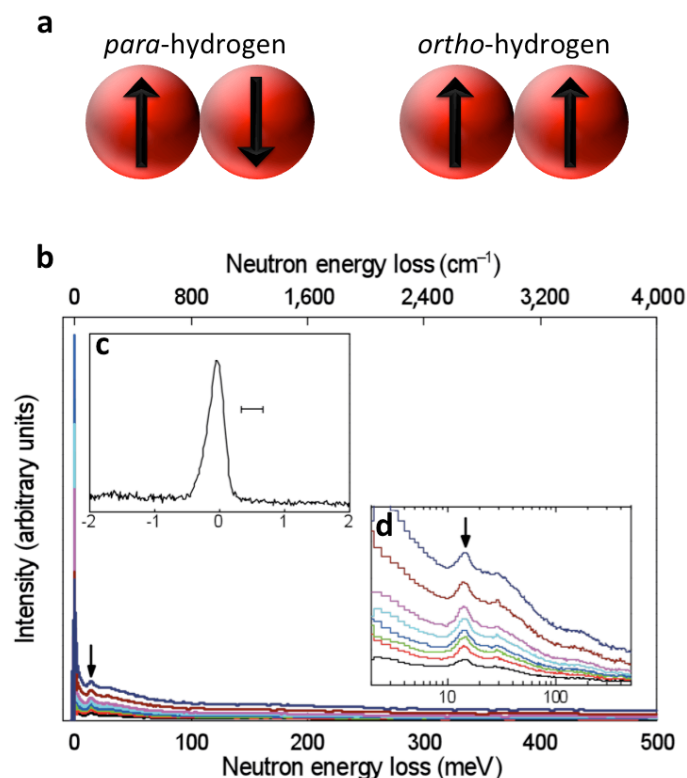

Figure 1. (a) The *para-* ($J = 0$) and *ortho-* ($J = 1$) spin isomers of hydrogen. (b) INS spectra for H_2 adsorbed on TE7 carbon beads at 77 K in order of ascending H_2 pressure (0.016-3.5 MPa). (c) Magnified elastic region (-2 to 2 meV) of the INS spectrum at the lowest pressure (0.016 MPa); the bar represents the instrumental FWHM resolution. (d) Magnified region of the INS spectra showing the rotor line at 14.7 meV, plotted on a logarithmic scale on the *x*-axis.

While INS measurements are typically performed at temperatures below 25 K to maximize resolution of the vibrational spectra,[12,13] here we combined INS measurements with volumetric gas sorption experiments to probe the phase behaviour of supercritical hydrogen at 77 K (a temperature that is more practically relevant for H_2 storage applications) in a nanoporous carbon material and show direct physical evidence for an accumulation of solid-like H_2 in the pores.

The INS measurements were only possible due to modifications to the TOSCA instrument at the ISIS neutron facility, which enabled measurement at high resolution ($\Delta E / E < 1.25$ %, where E is the energy lost by the incoming neutron) over the widest range of energy transfer of any INS instrument in the world. The improved high resolution at low energies allowed quantitative analysis of the elastic region of a scattering spectrum (where little or no energy is transferred between the incident neutron and the target H_2 molecule) as a function of gas pressure, with simultaneous monitoring of the inelastic regions, to provide information on the state (gaseous, liquid or solid) of the H_2 in the pores. INS spectra were collected on H_2 dosed onto a standard reference material of TE7 activated carbon beads (from

MAST Carbon International, UK) at eight gas pressures (0.016, 0.070, 0.160, 0.301, 0.630, 0.998, 2.070, and 3.500 MPa), with ~12 h data collection periods. This material was selected as it presents a reasonably chemically-homogenous adsorbing surface, allowing unambiguous analysis of INS spectra, and has a modal nanopore diameter within the pore size range for maximizing interactions with H_2[14] (~0.7 nm as determined *via* N_2 sorption at 77 K – see Figure S1 in Supplementary Information). The chemical and structural properties of the TE7 carbon were thoroughly characterized[15] and the excess H_2 sorption isotherm for this material was measured at 77 K to a maximum pressure of 17 MPa (see Figure S2 in Supplementary Information). For the INS experiment, a room-temperature equilibrium mixture of *para*-H_2 ($J = 0$, where J is the rotational quantum number) and *ortho*-H_2 ($J = 1$) was used for the *in-situ* gas dosing at 77 K (see Figure 1a). The use of so-called "normal hydrogen", which includes the *para* and *ortho* nuclear spin isomers of molecular hydrogen resulted in distinct characteristic features in both the elastic and inelastic regions of the neutron scattering spectrum. Due to the paramagnetic nature of activated carbons, the statistical population of *para*-H_2: *ortho*-H_2 at 77 K rapidly equilibrated to a 1:1 mixture in the sample.[16]

RESULTS AND DISCUSSION

The INS energy loss spectra of the H_2 in the pores at 77 K (Figure 1b) showed two important and remarkable features at each H_2 loading pressure measured. First, the intense, sharp peak at ~0 meV due to elastic scattering by *ortho*-H_2 indicated the presence of dense liquid- or solid-like hydrogen. While both condensed phases will show a sharp elastic scattering peak due to far higher densities of *ortho*-H_2 molecules than in the gas phase, the elastic peak from the more mobile liquid phase will typically be broadened relative to the same peak from solid H_2, as a result of quasielastic interactions. The full-width at half-maximum (FWHM) of the elastic peak of ~0.3 meV at the lowest adsorption pressure measured here (0.016 MPa H_2) remained approximately equal to TOSCA's instrumental peak resolution (indicated by the horizontal bar of width 0.3 meV in Figure 1c), taking into account the significant contributions from multiple-scattering and self-shielding from the >10 cm³ sample size, suggesting that the H_2 contributing to this peak had limited mobility. A full analysis of the FWHM of the elastic line is provided in the Supplementary Information (see Figures S3 and S4). The second prominent feature present in all of the spectra was a well-resolved peak at ~14.7 meV (Figure 1d), which is only present for the *para*-to-*ortho* transition in immobilized H_2.[12,13,17,18] This peak (commonly referred to as the "rotor line", as it corresponds to the free, unperturbed rotation of molecular H_2) denotes the presence of H_2 that is strongly pinned in all three dimensions and lacks translational freedom to recoil. It is not present in the INS spectra for either bulk liquid or gaseous *para*-H_2 (see Figure S5 in Supplementary Information), and indicates a population of solid-like H_2 which systematically increases with increasing H_2 loading pressure. A full analysis of the FWHM of the rotor line is provided in the Supplementary Information (see Figure S6 and S7). The 14.7 meV rotor line was also confirmed to also be present in the INS spectrum of the same material dosed

2

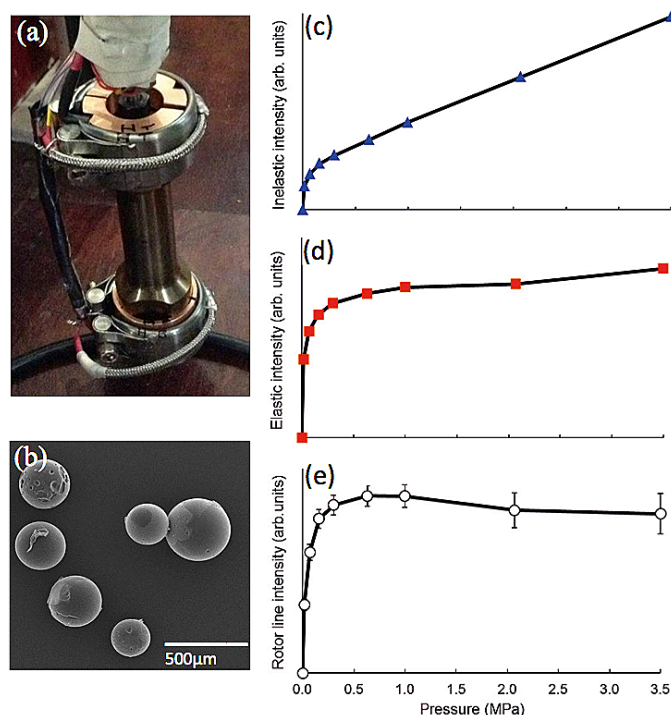with H_2 at a temperature of 100 K (see Figure S8 in Supplementary Information).

Figure 2. (a) The high pressure cryogenic cell used in the INS experiments. (b) SEM image of the morphology of the TE7 nanoporous carbon beads. (c) The total inelastic signal (integrated intensity from 2 meV to 500 meV) (d) Integrated intensity under the elastic peak from -2 meV to +2 meV. (e) Integrated intensity under the 14.7 meV rotor line which indicates the amount of solid-like H_2 present. Standard errors from the fit are shown, with standard errors for (c) and (d) within the size of the data markers. The data points are joined by straight lines as guides to the eye.

As the total neutron scattering intensity in each INS spectrum was normalized to the number of neutron counts, the integrated intensities under the peaks over different regions of the spectrum could be evaluated to determine relative amounts of H_2 in different states as a function of H_2 dosing pressure (Figure 2). The total integrated intensity over the entire inelastic range (2-500 meV) was dominated by the contribution from gaseous H_2 in and around the sample and increased linearly with pressure (Figure 2c), as would be expected from the gas equation of state.[1] The area under the elastic peak, determined by numerical integration from -2 meV to +2 meV after subtraction of a linear background and indicating the amount of H_2 in a strongly bound condensed state, increased rapidly at low pressures before starting to plateau at pressures >1 MPa (Figure 2d). The integrated intensity under the 14.7 meV rotor line, determined using a Gaussian peak shape after subtraction of a fourth-order polynomial background, corresponded solely to the amount of solid-like H_2 in the material. The presence of the 14.7 meV rotor line even at the very lowest pressures of H_2 studied (0.016 MPa) suggests direct accumulation of H_2 with solid-like characteristics, rather than a gaseous phase that increas-

es in density with increasing pressure. Figures 2d and 2e show the dependence of the integrated intensity of the rotor line with pressure matches that of the elastic peak within the uncertainty margins resulting from the lower count statistics of the lower-intensity rotor line. The closely mirrored profiles of the integrated intensities of the two independent peaks suggested strongly that the densification of both the *ortho-* and *para-*H_2 were a result of the same phenomenon and were due to the presence of the solid-like hydrogen.

The pressure dependence of the H_2 accumulation measured by INS was compared to amounts measured by volumetric gas sorption using a Sieverts-type apparatus at 77 K (Figure 3). The integrated intensity over the elastic region of the spectrum (chosen for comparison due to the superior count statistics) in arbitrary units was scaled to result in a least-squares best fit to the calculated weight percent of H_2 in the adsorbed phase from volumetric gas sorption measurements. The scaled INS integrated intensities were found to be strongly correlated to the calculated total amount of adsorbed H_2 expressed in weight percent relative to the dry, evacuated carbon sample (see Figure 3 and Tables S1 and S2 in Supplementary Information), with the concurrence of the onset of the plateau region in the INS intensities and the gas sorption data indicating that the accumulation of the solid hydrogen has an effective upper limit, which may signify the point at which the nanopores are completely filled with adsorbed H_2. The original and scaled data are in Tables S1 and S2 in Supplementary Information, along with details of the modelling.

Theoretical predictions of the density of the adsorbed H_2 (termed the "adsorbate") in the pores, using a development of earlier analysis[19,20] applied to the experimental high-pressure Gibbs excess isotherm (to 17 MPa) for H_2 adsorbed on the TE7 carbon beads at 77 K, was also consistent with the evidence from INS for the formation of solid-like H_2. The excess data was modelled using the Tóth equation[21] for adsorbate filling of the pore space, to yield an estimate of the density of the adsorbed H_2 phase (assumed constant) of 101 ± 2 kg m^{-3} (see Figure S2 in Supplementary Information). This is significantly higher than the maximum density of liquid H_2, 77 kg m^{-3} at the liquid-solid-vapour triple point (13.96 K and 0.00736 MPa)[1] and is closer to the density of bulk solid H_2, which is a highly compressible solid with densities >87 kg m^{-3}.[16]

The powerful combination of INS measurements and gas sorption analysis points to a bulk densification phenomenon that, while consistent with modelling (see, for example, the prediction of a "solid-like phase with densities higher than bulk solid hydrogen" from Dundar *et al.*'s modelling of supercritical hydrogen sorption on MOFs)[22] had not been previously observed experimentally. Past experimental observations consistent with localized regions of solid-like densities of adsorbed H_2 at elevated temperatures have generally been attributed to the strength of specific adsorption sites in MOFs and zeolites. For example, refinements of neutron diffraction data at 4 K indicate that some crystalline MOF materials support D_2-D_2 intermolecular separation distances that are shorter than the 0.36 nm found in solid H_2.[10,23-25] In these studies, the local surface densification of H_2 was ascribed to the strong interactions between the H_2 and the unsaturated metal centres in the frameworks. Similarly, H_2 rotor lines previously reported in INS spectra of zeolite sam-

ples at temperatures up to 70 K show a shift in energy, due to the influence of the strong binding of H_2 on specific adsorption sites.[18,26] Short range order and liquid-like behaviour of D_2 has also been predicted to exist in areas between metal
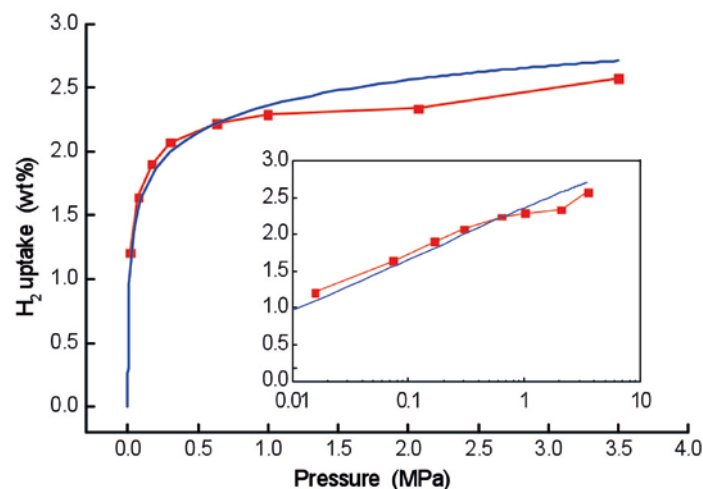

Figure 3. Scaled integrated intensity under the INS elastic peak from -2 meV to +2 meV with pressure (red squares joined by straight lines as guides to the eye, standard errors within the size of the data markers), and the amount of densified H_2 estimated from modelling of the experimental excess adsorption isotherm (solid blue line). Inset is the same data plotted using a logarithmic pressure scale.

sites in zeolites and MOFs at 50 K, to explain broadening effects in neutron diffraction patterns.[11] Carbon surfaces, however, are known to only have very weak interactions with H_2. The phenolic resin-derived TE7 carbons, in particular, have been shown via temperature programmed desorption to have only small proportions of surface oxygen groups, [27,28] meaning that they are likely to have limited surface functionality. This indicates that the pseudo-condensation of supercritical gas seen here at 77 K is instead due to confinement effects in optimally-sized nanopores.[14]

Comparative, single pressure (1 bar) H_2 dosing INS measurements on onion-like carbon nanomaterials (OLC-1750) having negligible proportions of nanopores less than 10 Å in diameter [29,30] show no such peak in the 14.7 meV region, supporting the hypothesis that the pore dimension is a critical factor. Similarly, while other activated carbon materials (TE7-20 and TE3 from MAST carbon) and AX-21 (Anderson Development Co) show small rotor peak contributions (see Supplementary Figure S9), the integrated intensity is not proportional to the total micropore volume, indicating that only a fraction of the micropores contribute to this effect and that a very narrow pore size distribution is required. This has been shown experimentally in the case of carbide-derived carbons,[31] for which higher than liquid H_2 densities were calculated from 77 K sorption isotherms for ~0.6 nm diameter pores.[32]

Molecular simulation and modelling of hydrogen in carbon nanomaterials seems to support the possibility of densification of adsorbed hydrogen to greater than liquid densities. For example, there have been estimates of adsorptive capacities from Grand Canonical Monte Carlo molecular simulations (with quantum effects estimated using the Feynman-Hibbs effective potential) and density functional theory (without the dispersion correction) that predicted elevated levels of densification for H_2 in 0.3 nm carbon slit pores and carbon nanotubes,[33,34] equating to densities in the region of 80 kg m^{-3} at 0.1 MPa and 77 K, while theoretical modelling of supercritical adsorption isotherms has predicted a transition to a solid-like phase of H_2 in activated carbon at 40 K.[35] Experimental room-temperature small-angle neutron studies of 0.9 nm pores in carbon have also estimated greater than liquid densities of H_2 at pressures of 20 MPa.[36]

Confinement effects are known to induce shifts in the phase transition temperatures for sub-critical adsorbed phases[37] and, thus, the pseudo-condensation of supercritical gas reported here could be a general phenomenon. It is, therefore, possible that the presence of the ~14.7 meV rotor line in INS studies of other highly nanoporous carbons at supercritical temperatures[38,39] is likely to be similarly indicative of the presence of densified solid-like H_2 (Supplementary Information, Figure S9). This is, however, the first time that the observation of this phenomenon has been correlated to gas sorption measurements and shown to be consistent with accumulation of solid-like H_2 with pressure.

CONCLUSION

Experimental evidence for a solid-like H_2 in the pores of TE7 carbon at 77 K clearly demonstrates the potential for further development of adsorptive hydrogen storage materials containing micropores of an optimum size. Due to its relatively low micropore volume (< 0.5 cm^3 g^{-1}, see Supplementary Information) the 3 wt% H_2 uptake of the TE7 material at 77 K and 17 MPa (which is ~80 % of the estimated maximum uptake at this temperature) remains low compared with the current US Department of Energy targets for onboard H_2 storage systems for vehicles[40] (7.5 wt% of useable H_2, based on the weight of the entire hydrogen storage system). However, a material with a much higher, and not unreasonable, micropore volume of 1.5 cm^3 g^{-1} which is 80 % filled with H_2 adsorbate of density 100 kg m^{-3}, would display an impressive uptake of 12 wt%. This compares favourably with the high observed H_2 uptake of 10 wt% in MOF NU-100 at 5.6 MPa and 77 K.[41] This work also counters the widely-held assumption of an upper limit of liquid-like adsorbed phase density, and, thus, will aid in advancing models for the evaluation of gas storage capacities in nanoporous materials, and could lead to the design of higher-capacity nanoporous adsorbents.

METHODS

The reference sample of TE7 activated carbon beads (sourced from MAST Carbon International, UK) was produced from a carbonized phenolic resin-based material activated at high temperature (750 °C) in a steam atmosphere. The BET nitrogen specific surface area at 77 K was measured to be 960±50 m^2 g^{-1} obtained from low pressure (up to 0.1 MPa) nitrogen sorption measurements at 77 K with a 60 min equilibration time.[15] The micropore volume, evaluated from the Dubinin-Radushkevich method is 0.43±0.03 cm^3 g^{-1}. The skeletal density of the sample was measured using a He pycnometer (Micromeritics AccuPyc1330) and was established as being 1.90±0.03 g cm^{-3}. The OLC-1750 carbon onions where synthesized by vacuum

annealing of detonation nanodiamond powder (Ray Technologies Ltd., Israel). Placed in a graphite crucible, the nanodiamond powder was annealed in vacuum (10^{-4} to 10^{-5} mbar) for 3 h at 1750 °C in a water-cooled high temperature furnace with tungsten heaters (Thermal Technology, USA).[29,30]

High-pressure (up to 20 MPa) hydrogen adsorption/desorption measurements were performed on a Hiden HTP-1 Sieverts-type volumetric gas sorption analyser with ultra- high purity (Air Products BIP-Plus, 99.99996 %) hydrogen at 77 K using a liquid nitrogen bath for temperature control. Prior to hydrogen uptake measurements the ~150 mg samples were degassed at 623 K for 8 h under a vacuum of 0.1 mPa prior to each isothermal measurement in order to remove moisture and desorbed gases from the surface. All isotherms were fully reversible and repeat isotherms for different samples were reproducible to within 0.3 % of measured amounts adsorbed.

The INS spectra were collected on the TOSCA inelastic neutron scattering beamline at the Rutherford Appleton laboratories in the UK, which has an energy window from -3 meV to +500 meV. The full-width at half-maximum instrumental resolution is 300 µeV over the range -3 meV to +3 meV (*i. e.*, in the elastic region) and in the range 3 to 500 meV the energy resolution is $\Delta E / E < 1.25$ %. A ~10 g sample of carbon was degassed *via* heating *ex-situ* at 623 K for 8 h under high vacuum (0.1 mPa), then loaded in an Ar glovebox into a high pressure (7 MPa) stainless steel sample can. Temperature control was supplied by a standard cryofurnace ancillary. Normal hydrogen gas (Air Liquide, 99.999 % purity) was dosed into the sample and thermally equilibrated at 77 K before the pressure was recorded using a baratron and a high-pressure transducer. The data were corrected for the presence of terminal H atoms in the carbon by subtraction of 12 h background scans of the degassed sample under dynamic vacuum at the measurement temperature (77 K). Note that the spectra for the degassed carbon sample did not show a peak at ~14.7 meV. Data were accumulated for 700 µA h, with up to three spectra being collected at each pressure over collection periods of 8-12 h (pressures = 0.016, 0.070, 0.160, 0.301, 0.630, 0.998, 2.070, and 3.500 MPa). The data processing and peak integration was performed using the Mantid software (available from http://www.mantidproject.org).

ASSOCIATED CONTENT

Supporting Information

Details of the materials characterization, experimental methods, raw data, analysis and modelling are available free of charge *via* the Internet at http://pubs.acs.org.

AUTHOR INFORMATION

Corresponding Authors

V.Ting@bath.ac.uk
T.J.Mays@bath.ac.uk

REFERENCES

1. Leachman, J. W.; Jacobsen, R. T.; Penoncello, S. G.; Lemmon, E. W., Fundamental Equations Of State For Parahydrogen, Normal Hydrogen, And Orthohydrogen. *J. Phys. Chem. Ref. Data* 2009, 38, 721-748.

2. Datchi, F.; Loubeyre, P.; Letoullec, R., Extended And Accurate Determination Of The Melting Curves Of Argon, Helium, Ice (H$_2$O) And Hydrogen (H$_2$). *Phys. Rev. B* 2000, 61, 6535-6546.

3. Deemyad, S.; Silvera, I. F., Melting Line Of Hydrogen At High Pressures. *Phys. Rev. Lett.* 2008, 100, 155701.

4. Schlapbach, L.; Zuttel, A., Hydrogen-Storage Materials For Mobile Applications. *Nature* 2001, 414, 353-358.

5. Van Den Berg, A. W. C.; Arean, C. O., Materials For Hydrogen Storage: Current Research Trends And Perspectives. *Chem. Commun.* 2008, 668-681.

6. Rouquerol, J.; Avnir, D.; Fairbridge, C. W.; Everett, D. H.; Haynes, J. H.; Pernicone, N.; Ramsay, J. D. F.; Sing, K. S. W.; Unger, K. K., Recommendations For The Characterization Of Porous Solids. *Pure Appl. Chem.* 1994, 66, 1739-1758.

7. Broom, D. P., Hydrogen Storage Materials: The Characterisation Of Their Storage Properties. Springer Science & Business Media: 2011.

8. Züttel, A.; Sudan, P.; Mauron, P.; Wenger, P., Model For The Hydrogen Adsorption On Carbon Nanostructures. *Appl. Phys. A-Mater.* 2004, 78, 941-946.

9. Rowsell, J. L. C.; Eckert, J.; Yaghi, O. M., Characterization Of H2 Binding Sites In Prototypical Metal-Organic Frameworks By Inelastic Neutron Scattering. *J. Am. Chem. Soc.* 2005, 127, 14904-14910.

10. Brown, C. M.; Liu, Y.; Neumann, D. A., Neutron Powder Diffraction Of Metal-Organic Frameworks For Hydrogen Storage. *Pramana J. Phys.* 2008, 71, 755-760.

11. Lee, H.; Choi, Y. N.; Choi, S. B.; Kim, J.; Kim, D.; Jung, D. H.; Park, Y. S.; Yoon, K. B., Liquid-Like Hydrogen Stored In Nanoporous Materials At 50 K Observed By In Situ Neutron Diffraction Experiments. *J. Phys. Chem. C* 2013, 117, 3177-3184.

12. Ramirez-Cuesta, A. J.; Jones, M. O.; David, W. I. F., Neutron Scattering And Hydrogen Storage. *Mater. Today* 2009, 12, 54-61.

13. Mitchell, P. C. H.; Parker, S. F.; Ramirez-Cuesta, A.; Tomkinson, J., Vibrational Spectroscopy With Neutrons : With Applications In Chemistry, Biology, Materials Science And Catalysis. World Scientific: Hackensack, NJ, 2005; P Xxvi, 642 P.

14. Gogotsi, Y.; Portet, C.; Osswald, S.; Simmons, J. M.; Yidirim, T.; Laudisio, G.; Fischer, J. E., Importance Of Pore Size In High-Pressure Hydrogen Storage By Porous Carbons. *Int. J. Hydrogen Energ.* 2009, 34, 6314-6319.

15. Hruzewicz-Kołodziejczyk, A.; Ting, V. P.; Bimbo, N.; Mays, T. J., Improving Comparability Of Hydrogen Storage Capacities Of Nanoporous Materials. *Int. J. Hydrogen Energ.* 2011, 37, 2728-2736.

16. Silvera, I. F., The Solid Molecular Hydrogens In The Condensed Phase - Fundamentals And Static Properties. *Rev. Mod. Phys.* 1980, 52, 393-452.

17. Young, J. A.; Koppel, J. U., Slow Neutron Scattering By Molecular Hydrogen + Deuterium. *Phys Rev. A-Gen. Phys.* 1964, 135, A603

18. Colognesi, D.; Celli, M.; Ramirez-Cuesta, A. J.; Zoppi, M., Lattice Vibrations Of Para-Hydrogen Impurities In A Solid Deuterium Matrix: An Inelastic Neutron Scattering Study. *Phys. Rev. B* 2007, 76, 174304.

19. Bimbo, N.; Ting, V. P.; Hruzewicz-Kołodziejczyk, A.; Mays, T. J., Analysis Of Hydrogen Storage In Nanoporous Materials For Low Carbon Energy Applications. *Faraday Discuss.* 2011, 151, 59-74.

20. Sharpe, J. E.; Bimbo, N.; Ting, V. P.; Burrows, A. D.; Jiang, D.; Mays, T. J., Supercritical Hydrogen Adsorption In Nanostructured Solids With Hydrogen Density Variation In Pores. *Adsorption* 2013, 19, 643-652.

21. Tóth, J., Gas-(Dampf-) Adsorption An Festen Oberflachen Inhomogener Aktivitat .1. *Acta Chim. Hung.* 1962, 30, 415.

22. Dundar, E.; Zacharia, R.; Chahine, R.; Benard, P., Performance Comparison Of Adsorption Isotherm Models For Supercritical Hydrogen Sorption On MOFs. *Fluid Phase Equilib.* 2014, 363, 74-85.

23. Liu, Y.; Kabbour, H.; Brown, C. M.; Neumann, D. A.; Ahn, C. C., Increasing The Density Of Adsorbed Hydrogen With Coordinatively Unsaturated Metal Centers In Metal−Organic Frameworks. *Langmuir* 2008, 24, 4772-4777.

24. Yildirim, T.; Hartman, M. R., Direct Observation Of Hydrogen Adsorption Sites And Nanocage Formation In Metal-Organic Frameworks. *Phys. Rev. Lett.* 2005, 95.

25. Luo, J.; Xu, H.; Liu, Y.; Zhao, Y.; Daemen, L. L.; Brown, C.; Timofeeva, T. V.; Ma, S.; Zhou, H.-C., Hydrogen Adsorption In A Highly Stable Porous Rare-Earth Metal-Organic Framework: Sorption Properties And Neutron Diffraction Studies. *J. Am. Chem. Soc.* 2008, 130, 9626-9327.

26. Ramirez-Cuesta, A. J.; Mitchell, P. C. H. Hydrogen Adsorption In A Copper ZSM5 Zeolite: An Inelastic Neutron Scattering Study *Catal. Today* 2007, 120, 368-373

27. Pigamo, A.; Besson, M.; Blanc, B.; Gallezot, P.; Blackburn, A.; Kozynchenko, O.; Tennison, S.; Crezee, E.; Kapteijn, F., Effect Of Oxygen Functional Groups On Synthetic Carbons On Liquid Phase Oxidation Of Cyclohexanone. *Carbon* 2002, 40, 1267−1278

28. Figueiredo, J. L.; Pereira, M. F. R.; Freitas, M. M. A.; Orfao J. J. M., Modification Of The Surface Chemistry Of Activated Carbons. *Carbon* 1999, 37,1379−1389

29. Zeiger, M.; Jäckel, N.; Aslan, M.; Weingarth, D.; Presser, V., Understanding Structure And Porosity Of Nanodiamond-Derived Carbon Onions. *Carbon* 2015, 84, 584-598.

30. McDonough, J. K.; Frolov, A. I.; Presser, V.; Niu, J.; Miller, C. H.; Ubieto, T.; Fedorov, M. V.; Gogotsi, Y., Influence Of The Structure Of Carbon Onions On Their Electrochemical Performance In Supercapacitor Electrodes. *Carbon* 2012, 50, 3298-3309.

31 .Gogotsi, Y.; Dash, R. K.; Yushin, G.; Yildirim, T.; Laudisio, G.; Fischer, J. E., Tailoring Of Nanoscale Porosity In Carbide-Derived Carbons For Hydrogen Storage. *J. Am. Chem. Soc.* 2005, 127, 16006-16007.

32. Yushin, G.; Dash, R.; Jagiello, J.; Fischer, J. E.; Gogotsi, Y., Carbide-Derived Carbons: Effect Of Pore Size On Hydrogen Uptake And Heat Of Adsorption. *Adv. Funct. Mater.* 2006, 16, 2288-2293.

33. Jagiello, J.; Anson, A.; Martinez, M. T., DFT-Based Prediction Of High-Pressure H_2 Adsorption On Porous Carbons At Ambient Temperatures From Low-Pressure Adsorption Data Measured At 77 K. *J. Phys. Chem B* 2006, 110, 4531-4534.

34. Wang, Q. Y.; Johnson, J. K., Molecular Simulation Of Hydrogen Adsorption In Single-Walled Carbon Nanotubes And Idealized Carbon Slit Pores. *J. Chem. Phys.* 1999, 110, 577-586.

35. Dundar, E.; Zacharia, R.; Chahine, R.; Bénard, P., Modified Potential Theory For Modeling Supercritical Gas Adsorption. *Int. J. Hydrogen Energ.* 2012, 37, 9137-9147.

36. Gallego, N. C.; He, L. L.; Saha, D.; Contescu, C. I.; Melnichenko, Y. B., Hydrogen Confinement In Carbon Nanopores: Extreme Densification At Ambient Temperature. *J. Am. Chem. Soc.* 2011, 133, 13794-13797.

37. Peterson, B. K.; Walton, J. P. R. B.; Gubbins, K. E., Fluid Behavior In Narrow Pores. *J. Chem. Soc. Farad. T. 2* 1986, 82, 1789-1800.

38. Brown, C. M.; Yildirim, T.; Neumann, D. A.; Heben, M. J.; Gennett, T.; Dillon, A. C.; Alleman, J. L.; Fischer, J. E., Quantum Rotation Of Hydrogen In Single-Wall Carbon Nanotubes. *Chem. Phys. Lett.* 2000, 329, 311-316.

39. Ren, Y.; Price, D. L., Neutron Scattering Study Of H_2 Adsorption In Single-Walled Carbon Nanotubes. *Appl. Phys. Lett.* 2001, 79, 3684-3686.

40. US Department of Energy, Explanations Of Freedomcar/DOE Hydrogen Storage Technical Targets, Available From http://www1.eere.energy.gov/hydrogenandfuelcells//pdfs/freedomcar_targets_explanations.pdf.

41. Farha, O. K.; Yazaydin, A. O.; Eryazici, I.; Malliakas, C. D.; Hauser, B. G.; Kanatzidis, M. G.; Nguyen, S. T.; Snurr, R. Q.; Hupp, J. T., De Novo Synthesis Of A Metal-Organic Framework Material Featuring Ultrahigh Surface Area And Gas Storage Capacities. *Nat. Chem.* 2010, 2, 944-948.